Yan, S., Ma, Q. & Cheng, X. (2012). Numerical investigations on transient behaviours of two 3-D freely floating structures by using a fully nonlinear method. Journal of Marine Science and Application, 11(1), pp. 1-9. doi: 10.1007/s11804-012-1099-0

CITY UNIVERSITY LONDON

EST 1894

City Research Online

Numerical Investigations on Transient Behaviours of Two 3D Freely Floating Structures by using a fully nonlinear method

YAN S.[1], MA Q.W.[1*], CHENG Xiaoming[2]

[1]School of Engineering and Mathematical Sciences, City University London, United Kingdom
[2]GL-Noble Denton UK, London, United Kingdom

Abstract: Two floating structures in close proximity are very commonly seen in offshore engineering. They are often subjected to steep waves and, therefore, the transient effects on their hydrodynamic features are of great concern. This paper uses the quasi arbitrary Lagrangian-Eulerian finite element method (QALE-FEM), based on the fully nonlinear potential theory (FNPT), to numerically investigate the interaction between two three-dimensional (3D) floating structures, which undergoes motions with 6 degrees of freedom (DOFs), and are subjected to waves with different incident angles. The transient behaviours of floating structures, the effect of the accompanied structures and the nonlinearity on the motion of and the wave loads on the structures are the main focuses of the study.

Keywords: Fully nonlinear interaction; two floating structures; transient behaviours; potential flow; QALE-FEM method
CLC number:　　　**Document code:**　　　**Article ID:**

1 Introduction

In reality, one floating structure is often moored to another side by side with relatively small gap in between. A typical example is that a liquefied natural/petroleum gas (LNG/LPG) carrier is moored near a floating production storage and offloading system (FPSO) during their loading/offloading process. A standard procedure [e.g. The International Association of Classification Societies (2006)] is commonly applied to estimate the motion of and the force acting on the structures during the design, classification and inspection process. However, severe structure damages are still frequently reported [Smith (2007)]. This may indicate some uncertainties associated the standard procedure. The uncertainties may arise from the simplification on the wave/current conditions and the structure performance [Ma and Yan (2009) and Yan et al (2011a)]. For the problems with two structures arranged with small gap and subjected to steep waves, a number of simplifications made in the standard procedure will be discussed below.

The first simplification is to assume that the wave is periodic and uniform, the ship motion and the wave load are in steady state, ignoring the transient effects. A typical example in the standard procedure is that the motion response amplitude of operators (RAOs) is

adopted to evaluate the motion of the structures. The RAOs can only represent the motion magnitude in steady state [Ma and Yan (2009)]. However, the structures are likely to be exposed to varying waves. There are always transient responses whenever the waves propagating to them are changed. Ignoring the transient effects may lead to underestimation of the maximum motion magnitude as indicated by Ma and Yan (2009). Corresponding studies on the transient responses of floating structures to steep waves are rare, in particular by using fully nonlinear methods.

The second simplification often made is to assume two 3D structures in close proximity to be two-dimensional (2D) [e.g. Maiti & Sen(2001), Koo & Kim (2007) and Wang et al. (2011)]. This may be acceptable for the cases with two long structures with similar sizes. In general, the two structures may have quite different sizes – one perhaps being considerable larger than the other. As revealed by Yan et al (2011a), who compare 2D and 3D results of hydrodynamic forces on two closely located structures due to forced heaving motion, 2D analysis can leads to very different results from 3D analysis.

Furthermore, the nonlinearity is often either fully or partially ignored in the standard procedure. Even it is taken into account, the results based on 2nd-order disturbance theory are usually applied [Kashiwagi et al (2005), Sun, Eatock Taylor and Taylor (2010)]. It has been concluded that the nonlinearity in such problems is

important, particularly when the width of the gap is small, as confirmed by many experimental and numerical investigation, e.g. Kristiansen and Faltinsen (2008), Ma and Yan (2009), Sun, Eatock Taylor and Taylor (2010). Although the 2nd-order disturbance theory may give acceptable results, previous studies based on fully nonlinear 3D simulations addressing multiple structures [Ma and Yan (2009), Yan et al. (2008, 2011a,b)] has identified that the 3rd-order and higher-order components of forces and motions are considerably large in many cases. Limited comparisons in Yan et al (2011a,b) have also suggested that even based on 3rd-order approximation, the wave loads on structures may also be underestimated. Therefore, it is necessary to further study the nonlinearity associated with two structures in close proximity.

In this paper, the transient behaviours of two 3D floating structures in close proximity with motions of 6 DOFs will be investigated by using the FNPT-based QALE-FEM method. This method has been applied to studying multiple structures in waves covering: (1) the responses of two Wigley Hulls with relatively wide gap between them to steep waves [Yan and Ma (2008) and Ma and Yan (2009)]; (2) the forces and radiation coefficients of two heaving structures in close proximity [Yan and Ma (2011a)]; and (3) wave motions in the gap of two structures [Yan and Ma (2011b)]. In this paper, we will continue the study in this direction but will focus on the motions of and the wave loads on two floating structures subjected to steeper waves. The significance of the transient effects will be discussed. The nonlinearity, not only due to the wave amplitude but also due to the appearance of the accompanied structure, will be investigated.

2 Descriptions of numerical method

The numerical investigation is carried out in a numerical tank with mean water depth of *d*. A Cartesian coordinate system is used with the *oxy* plane on the mean free surface, the *x*-axis pointing from the left end to the far end wall and the *z*-axis being positive upwards. Only flat seabed is considered in this study.

In the QALE-FEM method, the flow in the tank is governed by the FNPT model where a boundary value problem for velocity potential ϕ is solved using the FEM. The Bernoulli's equation is used to find the force acting on bodies. The time derivative of velocity potential ($\partial\phi/\partial t$) in the Bernoulli's equation is also evaluated by solving a similar boundary value problem. The details of the FEM formulation have been discussed in our previous publications, for example Ma et al. (2001). Two main differences between the QALE-FEM method and the

conventional FEM method (Ma et al., 2001) are (1) the unstructured mesh is moving during the calculation by using a novel methodology based on the spring analogy method but purpose-developed for wave-structure interaction problems; (2) fully nonlinear free surface conditions are written in arbitrary Lagrangian-Eulerian forms. In addition, this method is also equipped with other three purpose-developed techniques necessary for modelling floating structure motions in large waves: (1) a three-point method for computing the velocity on the free surfaces and body surfaces suitable for unstructured/moving meshes; (2) the modified semi-implicit time integration method for floating bodies (ISITIMFB-M), with which the difficulty associated with wave-body coupling is solved; and (3) special technique for coping with wave overturning and impacting. These techniques ensure high robustness of the QALE-FEM. The details of those techniques will not be repeated here. Readers are referred to Ma and Yan (2006, 2009) and Yan and Ma (2007, 2010).

3 Numerical results and discussions

3.1 Model configuration and nondimensionlisation
In this section, the QALE-FEM method is used to model the fully nonlinear interaction between two 3D floating structures in steep waves. For simplification, rectangular cylindrical barge-type floating structures are used here. The model parameters are listed in Table 1. The water depth *d* is assumed to be 100m.

Table 1: Floating structure parameters

	Barge 1	Barge 2
Length (L_b)	180m	250m
Breadth (B_b)	30m	40m
Depth (D_b)	18m	23m
Draft (D_r)	10m	15m
Displacement	55350te	154750te
Centre of Gravity(G_c)	9m	11m
Radius of gyration in Roll	10m	13m
Radius of gyration in Pitch	45m	60m
Radius of gyration in Yaw	45m	60m

The mooring system is not a focus of this study and, therefore, is simplified as linear spring acting through the centre of the gravity. Under this simplification, the force due to mooring lines is approximated by using $k_m S_m$. in which k_m is the stiffness of the mooring line and is taken as 0.125 $\rho g d^2$ and 0.346 $\rho g d^2$ for Barge 1 and 2 respectively, where *g* is the gravitational acceleration; S_m is the displacement of the floating structure. Considering the fact that real berthing system normally applies strong moment in yaw direction in the cases with two structures moored side by side, the yaw motion is not

interested and restricted by applying a large artificial damping corresponding to this mode.

The incident monochromic waves are generated by a piston wavemaker which is mounted at the left end of the tank and undergoes a motion with displacement of $-a_w\cos(\omega t)$, where ω is the wave frequency; a_w is the amplitude estimated from the expected wave height (a) using the wavemaker transfer function [Dean and Dalrymple(1991)]. The floating structures are located in the centre of the tanks side by side and Barge 2 is located in the starboard of Barge 1. The width of the gap (B_g) between two barges is 0.15d, half of the breadth of Barge 1. Incident angle of waves to these barges are varied to make it equivalent to floating structures subjected to oblique waves. The incident angle in this investigation ranges from 0^0 (head sea) to 90^0 (beam sea).

For convenience, unless mentioned, otherwise, in the rest part of the paper, the parameters with a length scale are nondimensionalised by d; the time and frequency, by $\sqrt{d/g}$ and , $\sqrt{g/d}$ respectively; the force by $\rho g d^3$.
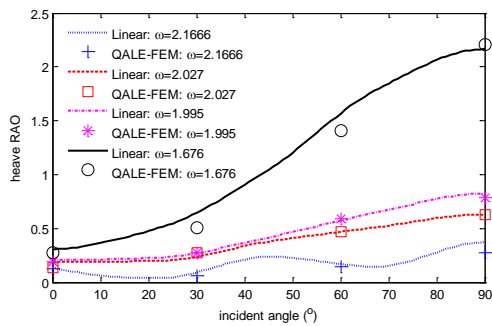

Fig. 1 Heave RAO of Barge No.1 subjected to oblique waves (B_g =0.15; Barge No.2 is fixed and Barge No.1 can only be allowed to move in heave direction)

3.2 Numerical accuracy and convergence
The accuracy of the QALE-FEM for the response of a single structure in head sea has been validated by Ma and Yan (2009). For the cases with two floating structures in close proximity, both the radiation coefficients [Yan and Ma (2011a)], heave RAO and wave elevation in the gap [Yan and Ma(2011b)] have been compared with corresponding results from other numerical methods. Satisfactory agreements have been achieved. All these comparisons have shed light on the promising accuracy of the QALE-FEM in the responses of two floating structures in steep waves. These will not be repeated here. For completeness, a result for one case is presented in Fig.1, where the heave RAO of Barge No.1 subjected to oblique waves in the cases where barge No.2 is fixed and Barge No.1 can only be allowed to move in heave direction, are compared with the linear results by using AQWA software. In this figure, the result from the

QALE-FEM is the component with the frequency of incoming waves obtained by FFT analysis to be consistent with linear results by AQWA.

In the QALE-FEM, a principle to determine the time step size based on the mesh size has been established in Yan and Ma (2010). Therefore, the convergence property in such cases is determined by the mesh size. For all cases presented in this paper, the representative mesh size ds on free surface is assigned to be $\lambda/30$ for the area away from the floating bodies, where λ is the incident wavelength. It is reduced to min($\lambda/180$, $L_b/200$) near the body surface; For the elements away from the free surface and the body surface, ds gradually increases following exponential principle as given in Ma et al (2001). The comparison on the results from this mesh resolution and another one with finer mesh (half of the mesh size) showed that the relative difference in harmonics up to 3rd-order is less than 1%. To save the space, discussion on the convergence tests will not be given here.

3.3. Transient test and natural frequencies
In the problem addressed here, the natural frequencies of structure motions need to be considered. In addition, the water in the gap between two structures may be initiated to have sloshing-like motion with their own the natural frequency [Wang et al (2011)]. Such natural frequency is also important for the behaviour of structures. Hereafter, we use natural frequency or natural frequencies to refer the natural frequency (-ies) of structure motions while the natural frequency of water oscillations in the gap is denoted by 'gap natural frequency. For the structure configuration adopted here, the gap natural frequency is close to 2 [Yan et al (2011a)]. To determine the natural frequencies of structure motions with effects of the damping and the effect of the accompanied structure, transient tests are firstly carried out in this subsection.

In the transient tests, one structure is given an initial velocity for specific motion mode and the other one is fixed. For example, in the transient test for roll motion of Barge 1, Barge 2 is fixed and Barge 1 is given an initial roll velocity of 0.01. The test is carried out in still water and no incident waves/currents are presented in the tank. The motion will be dissipated by intrinsic damping and a long-period oscillation corresponding to the roll natural frequency will be found as illustrated in Fig.2(a). Similarly, we can get the transient time histories of other motion modes as shown in Fig. 2(b). By using the FFT, the natural frequencies can be determined. According to the transient tests, the surge, sway, heave, roll and pitch natural frequencies for Barge 1 are 1.42, 1.06, 2.58, 0.57 and 1.02, respectively,. It should be noted that the motion natural frequency in the case with the accompanied structure may be slightly different from that without the accompanied structure, as demonstrated in Fig.3, which compares the sway motion histories in the transient tests for Barge 1 in the cases with fixed Barge 2 and without Barge 2.
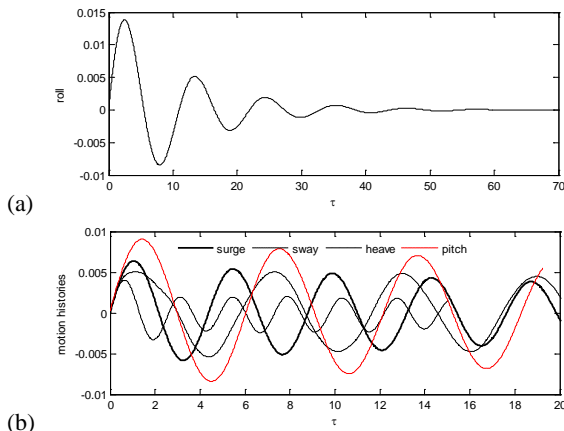
(a)

(b)

Fig. 2 Time histories of transient roll motion (a) and other motion modes(b) for Barge 1(B_g=0.15, Barge 2 is fixed)
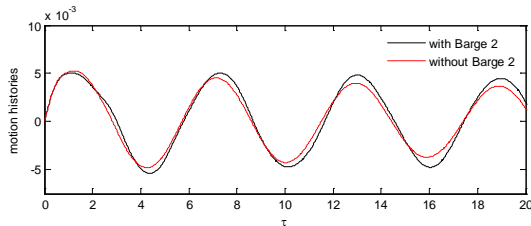

Fig. 3 Time histories of transient sway motion for Barge 1 in the cases with and without Barge 2.

3.4 Transient responses of floating structures

The transient responses of floating structures are discussed in this section. In the first case considered, the wave amplitude a is taken as 0.02 and the wave frequency ω equals 1.676. Fig.4 plots snapshots of the floating structures and the free surface elevations around the structures for illustrations.

The time histories of the motions of two structures under waves with different incident angles are recorded and analysed. A typical feature of the motion observed in the investigation is that the time histories of all motion modes have long-period oscillations before it become steady as demonstrated in Fig.5, which shows the surge time histories of two barges in the cases with 30^0 incident angle. From Fig.5, one may find that the period of such oscillation is roughly 24, corresponding to the frequency difference between the wave frequency (1.676) and the surge natural frequency (1.42). Similar phenomenon is also found in other cases. It, therefore, may be envisaged that the components corresponding to the motion natural frequency may play an important role.
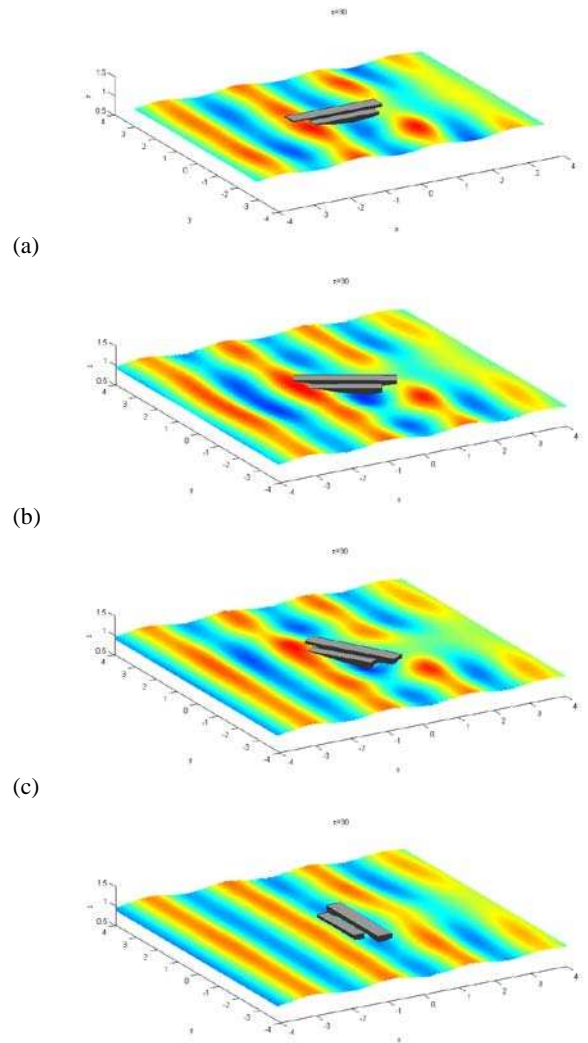

(a)

(b)

(c)

(d)

Fig. 4 Free surface profiles at $\tau \approx 30.0$ for (a) head sea; (b) 30° incident angle; (c) 60° incident angle and (d) beam sea (a=0.02, ω=1.676, B_g=0.15)

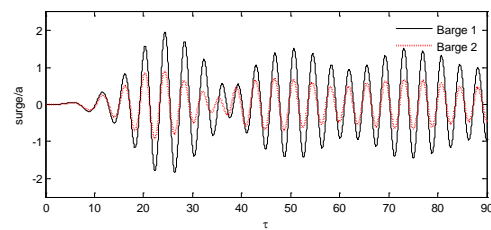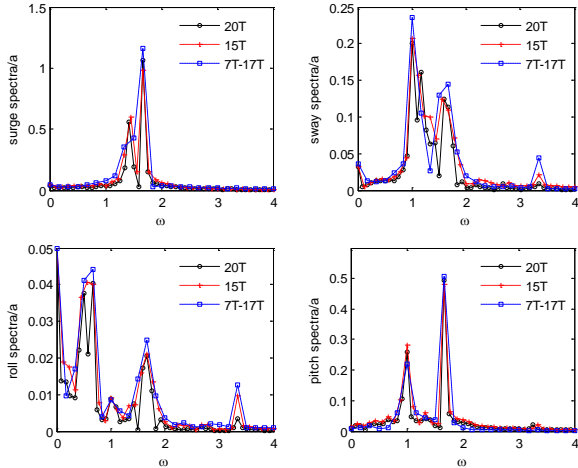Fig. 5 Time histories of surge of two barges in the case with 30° incident angle (a=0.02, ω=1.676, B_g=0.15)

Fig.6 Spectra for (a) surge, (b)sway, (c) roll and (d) pitch motions of Barge 1 in the case with 30° incident angle (a=0.02, ω=1.676, B_g=0.15)

To confirm this and to quantify the contributions of different components to transient motions, the motion spectra are evaluated by using the FFT. Some results are plotted in Fig.6 for the cases shown in Fig.5 but include more motion modes. In each figure in Fig.6, there are three groups of spectra, corresponding to results obtained by applying FFT analysis to different windows of time histories. For these two curves with legends of 20T and 15T, the window of time histories starts from the instant when the incident wave reaches the front of the floating structures and covers time durations of 20T and 15T, respectively, where T is the incoming wave period. The third one is based on the window of time histories starting from 7th wave periods with duration of 10T. Overall, the agreement between those results is acceptable. This suggests that different windows of time histories do not lead to considerably different results.

As observed from all motion modes shown in Fig.6, there are components corresponding to the wave frequency (1.676). These components are referred to as fundamental components ($S_{(1)}$) which provide a close estimation for motion RAOs as demonstrated in Fig. 1. Apart from this, a significant peak occurs at the frequency corresponding to the natural frequency, i.e. 1.42 for surge (Fig.6a), 1.06 for sway (Fig.6b), 0.57 for roll (Fig.6c) and 1.02 for pitch (Fig.6d). Similar phenomena have also found in the cases with different wave frequencies as illustrated in Fig.7. For convenience, this motion component corresponding to natural frequency is referred to as S_n. As shown in Fig.6, the magnitude of S_n is about 50% of the corresponding fundamental component for the surge motion(Fig.6(a) and Fig.6(d). For some motion modes such as sway (Fig.6(b)) and roll (Fig.6(c)), it may be twice as large the value of corresponding fundamental component. In the latter case, the main oscillation frequency observed in the transient time history is not the wave frequency but the natural frequency (for example the roll time histories shown in Fig.8, corresponding to

different incident wave angles, demonstrate the main frequency of roll motion is closed to its natural frequency 0.57 and far from the wave frequency of 1.676). This is also true for other wave frequencies tested and some results associated with the sway and roll motions corresponding to different wave frequencies are presented in Fig.9.
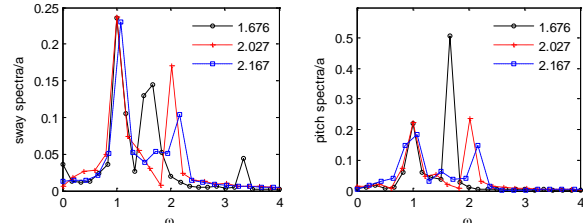

Fig.7 Spectra for (a)sway and (b) pitch motions of Barge 1 in the case with different wave frequencies(30° incident angle, a=0.02, B_g=0.15)
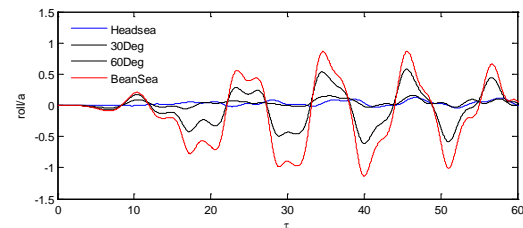

Fig. 8 Roll time histories of Barge 1 in the case with different incident angles (a=0.02, ω=1.676, B_g=0.15)
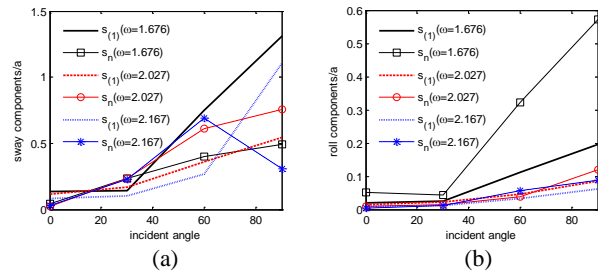

Fig.9 Fundamental component ($S_{(1)}$) and S_n of (a) sway and (b) roll in the cases with different incident angle(a=0.02, B_g=0.15)

In the spectra of roll motion, shown in Fig.6, except for the peaks corresponding to $S_{(1)}$ and S_n, one may find another peak between them, at $\omega \approx 1$ in Fig.6(c). This corresponds to natural frequencies of sway and pitch. In order to demonstrate the relationship between this peak and other motion modes, results corresponding to different incident wave angles and frequencies are shown in Fig. 10. It can be seen that the peak magnitudes at $\omega \approx 1$ do not only appear but are much larger than those at the wave frequency and roll natural frequency in the cases for beam sea. This indicates that the transient roll motion is strongly affected by sway or pitch. This is quite interesting. According to our numerical tests, if there would be no Barge 2, the roll motion under beam sea is not so significantly affected by sway and pitch. The phenomenon seen in this figure may be related to the effect of Barge 2 on Barge 1. This point will be further
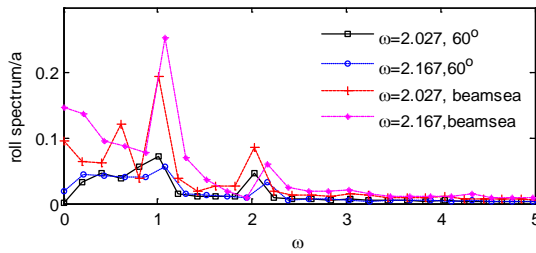
discussed in Section 3.6.

Fig. 10 Roll motion spectra of Barge 1 for the cases with different incident angles and frequencies (a=0.02, B_g=0.15)

(a)

(b)

(c)

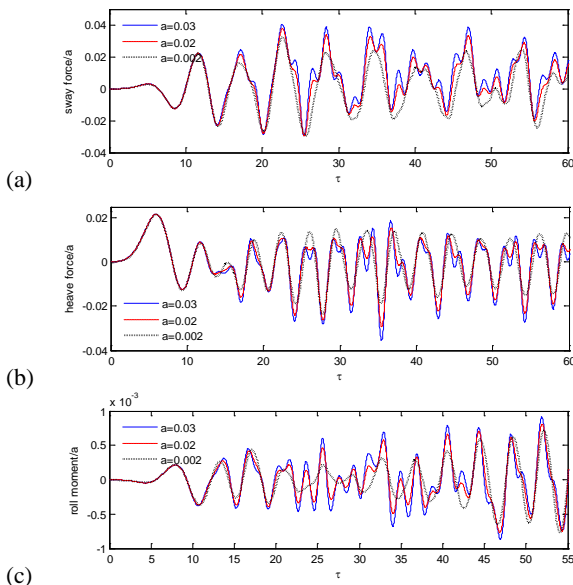Fig. 11 Time histories of (a) sway force, (b) heave force and (c) roll moments acting on Barge 1 in the cases with different wave amplitudes (30° incident angle, B_g=0.15, ω=1.676)

3.5 Nonlinear analysis of wave forces and moments
As indicated above, the nonlinearity plays important role in the problems with two floating structures in steep waves. A typical feature of nonlinearity shown in the time histories of motions or wave loads is the appearance of high-frequency oscillations. Fig.11 displays an example of the time histories of sway force, heave force and roll moments acting on Barge 1 subjected to the waves with different wave amplitudes. Obviously, the high-frequency oscillations are not found in the cases with very small wave amplitude, e.g. a=0.002 while as the wave amplitude increases, they become more significant. To further look at how important the nonlinearity is, the force / moment spectra in the cases shown in Fig.11 are produced by using FFT analysis and are plotted in Fig.12.

As observed from Fig.12, the fundamental component with ω=1.676 decreases, while higher-order components become more significant, as the wave amplitude increases. For the larger wave amplitude, 2nd-order components

obtained by the fully nonlinear analysis (ω=3.352) are more significant for all force/moment components and may be larger than the fundamental component, e.g. sway force in the case with a = 0.03. This phenomenon challenges 2nd-order disturbance theory assuming the 2nd-order component to be one order smaller than the fundamental component. It is also found that the 3rd-order components (ω = 5.028) can be considerably large and its magnitude may reach 20% of the fundamental component. In some cases, 4th-order components are visibly identified (Fig.12a). Based on this, one may envisage that ignoring 3rd-order components may cause considerable loss of accuracy.

(a)

(b)

(c)

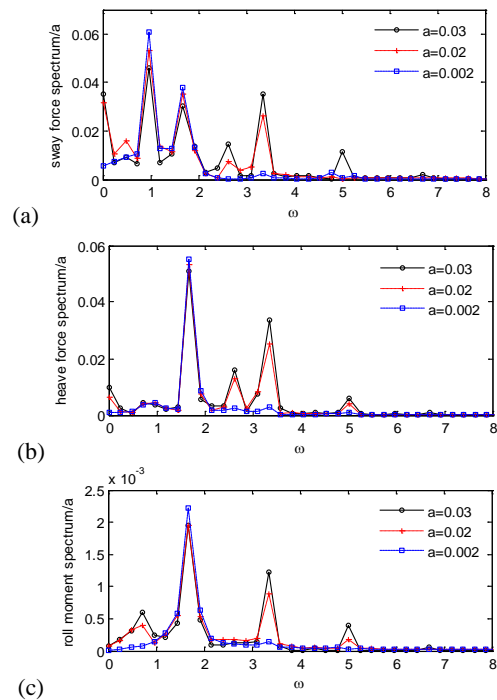Fig. 12 Spectra of (a) sway force, (b) heave force and (c) roll moments acting on Barge 1 in the cases with different wave amplitudes (30° incident angle, B_g=0.15, ω=1.676)

Fig.12 also shows that the component corresponding to the natural frequency may be significantly large due to the transient effects (e.g. the value at $\omega \approx 1.0$ in Fig.12a and the value at $\omega \approx 0.6$ in Fig.12c). Apart from the components indicated above, those near $\omega \approx 2.5$ are also considerable as shown in Fig. 21 (a) and (b). These may be due to the nonlinear interaction between the fundamental, linear and higher order components, since they have not be found in the case with smaller wave amplitude (a=0.002).

We have also analysed forces in the cases with other wave frequencies and incident angles and confirmed as being similar to what presented above, they are not included in this paper
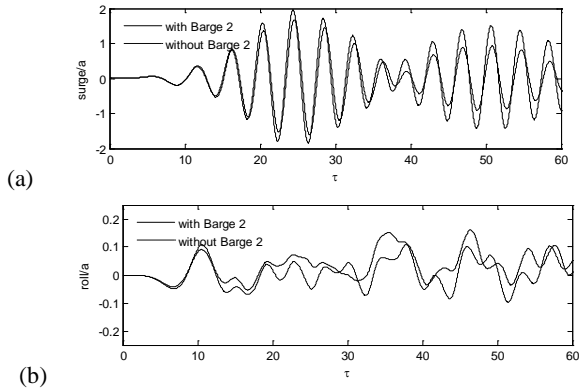
Fig. 13 Comparison of time histories of (a) surge and (c) roll of Barge No. 1 and the corresponding results without considering accompanied structure (*a*=0.02, *ω*=1.676, B_g=0.15, 30° incident angle)
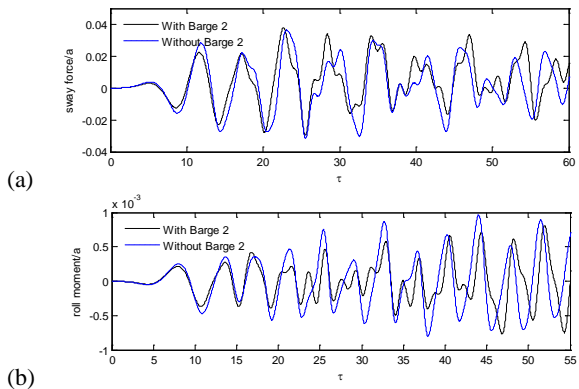

Fig. 14 Time histories of (a) sway force and (b) roll moment acting on Barge 1 in the cases with or without Barge 2(*a*=0.02, B_g=0.15, *ω*=1.676, 30° incident angle)
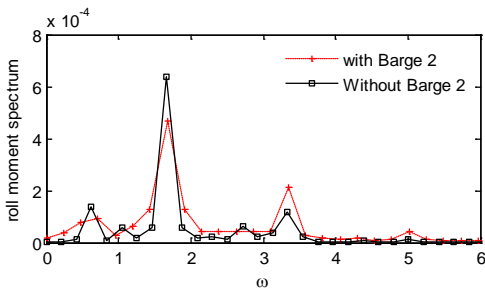

Fig. 15 Spectra of roll moments acting on Barge 1 in the cases with or without Barge 2 (30° incident angle, B_g=0.15, *ω*=1.676, *a*=0.02)

3.6 Effect of the accompanied structure

The effects of the accompanied structure on the behaviour of a floating structure are further studied. As an example, the effects of Barge 2 on the motion of or force on Barge 1 are discussed in this section. For comparison, cases without considering Barge 2 are run.

Motions of or wave loads (sway and roll) on Barge 1 in the cases with and without Barge 2 are compared. Considerable differences have been observed in all cases, e.g. those shown in Fig. 13 for structure motions and Fig. 14 for wave loads.

The accompanied Barge 2 does not only affect the magnitude of the motion or wave force on Barge 1, but also modifies the shape of the time history curve. Specifically, the time histories of the force/moment in the case with Barge 2 have larger high-frequency oscillations than those without Barge 2, as demonstrated in Fig. 15. In addition, the corresponding motion spectra shown in Fig. 16 suggests that in the case with Barge 2, the higher-order components, e.g. 2nd-order component (*ω*≈3.252) and 3rd-order component (*ω*≈5.028), are more significant than those in the case without Barge 2. A similar phenomenon may also be found in other cases with different frequencies and incident angels, as well as in the motion spectra (e.g. those shown in Fig. 16). This indicates that the accompanied structures nearby may make nonlinearity stronger, implying that the effects from the accompanied structure nearby should be taken into account.
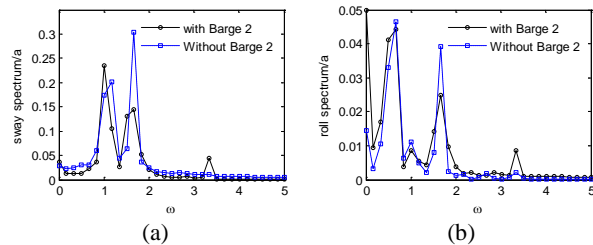

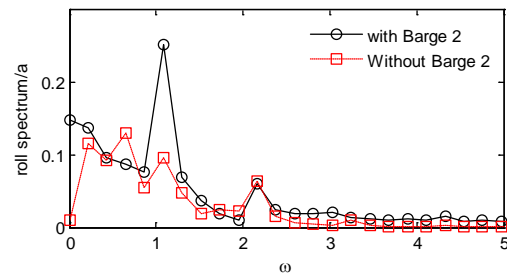Fig. 16 Sway(a) and roll(b) motion spectra of Barge 1 in the case with 30° incident angle; (*ω*=1.676, B_g=0.15)

Fig. 17 Roll motion spectra of Barge 1 for the cases with or without Barge 2 (*a*=0.02, B_g=0.15, Beam Sea, *ω*=2.167)

As mentioned in Section 3.5, influence of one motion mode (such as sway) on others (such as roll) may become stronger due to existence of the second structure. More evidences are provided here. Fig. 17 compares the roll motion spectra of Barge 1 subjected to beam sea in the cases with or without Barge 2. Clearly, in the case without Barge 2, the roll motion component corresponding to frequency *ω*≈1, i.e. the sway and pitch natural frequency, is significantly smaller than that in the case with Barge 2. Similar phenomenon has also been found for other motion modes in the cases with different incident angles.

4 Conclusions

In this paper, the QALE-FEM method is used to simulate the transient responses and wave loads of two floating structures subjected to waves with different incident angles. Both 3D structures undergo motion of 6DOFs. The motion of the structures and hydrodynamic force/moment acting on structures are investigated.

The results have indicated that (1) the transient effects are significant and, in many cases, cause considerably larger wave motion than that predicted by RAOs; (2) the accompanied structure in close proximity affects the motion of and force on the structures, makes nonlinearity stronger and enhances the interaction between different motion modes; (3) The 2nd-order component may be of similar significance to fundamental component. All results and conclusions suggest the necessity of using the fully nonlinear potential theory when investigating the responses and waves loads of two floating structures in close proximity.

Acknowledgement

References

Dean R.G., Dalrymple R.A.(1991) Water Wave Mechanics for Engineers and Scientists. World Scientific Publishing Co., ISBN 981-02-0420-5.

Hong S.Y., Kim J.H., Cho S.K., Choi Y.R., Kim Y.S. (2005). Numerical and experimental study on hydrodynamic interaction of side-by-side moored multiple vessels [J], Ocean Engng. 32: 783-801.

The International Association of Classification Societies (2006). Common Structural Rules for Bulk Carriers, January

Kashiwagi M., Endo K., Yamaguchi H (2005). Wave drift forces and moments on two ships arranged side by side in waves [J]. Ocean Engng. 32: 529-555.

Koo W.C., Kim M.H. (2007). Fully nonlinear wave-body interactions with surface-piercing bodies[J]. Ocean Engng. 34:1000-1012.

Kristiansen T., Faltinsen O.M. (2008) Application of a vortex tracking method to the piston-like behaviour in a semi-entrained vertical gap[J]. Applied Ocean Research, 30: 1-16.

Ma Q.W., Wu G.X., Eatock Taylor R. (2001) Finite element simulation of fully non-linear interaction between vertical cylinders and steep waves. Part 1: Methodology and numerical procedure[J]. Int J Numer Meth Fluids, 36: 265-285.

Ma Q.W., Yan S. (2006) Quasi ALE finite element method for nonlinear water waves[J]. J Comput Phys. 212:52-72.

Ma Q.W., Yan S. (2009) QALE-FEM for numerical modelling of nonlinear interaction between 3D moored floating bodies and steep waves[J]. Int J Numer Meth Engng , 78: 713-756.

Maiti S., Sen D. (2001)Nonlinear heave radiation forces on two-dimensional single and twin hulls, Ocean Eng, 28: 1031-1052.

Smith B.G, (2007). Extreme Waves and Ship Design. 10th International Symposium on Practical Design of Ships and Other Floating Structures Houston, Texas, United States of America.

Sun L., Eatock Taylor R., Taylor P.H. (2010). First and Second Order Analysis of Resonant Waves between Adjacent Barges[J] Journal of Fluids and Structures, 26:954-978.

Wang C.Z., Wu G.X., Khoo B.C. (2011) Fully nonlinear simulation of resonant motion of liquid confined between floating structures [J] Computer & Fluids, 44:89-101.

Yan S., Ma Q.W. (2007) Numerical simulation of fully nonlinear interaction between steep waves and 2D floating bodies using the QALE-FEM method [J]. J Comput Phys. 221: 666-692.

Yan S., Ma Q.W. (2008). Numerical Investigations on Responses of Two Moored 3D Floating Structures to Steep Waves. Proc Int Offshore and Polar Engng Conf (ISOPE2008), Vancouver, Canada, 322-310.

Yan S., Ma Q.W. (2010) QALE-FEM for modelling 3D overturning waves[J]. Int J Numer Meth Fluid , 63: 743-768.

Yan S., Ma Q.W., Cheng X. (2011a). Fully Nonlinear Hydrodynamic Interaction between Two 3D Floating Structures in Close Proximity[J], J. Int. Offshore and Polar Engng.,21:178-185.

Yan S., Ma Q.W., Cheng X. (2011b). Fully nonlinear simulation of two floating structures in close proximity subjected to oblique waves. Proc. Int. Offshore and Polar Engng. Conf. (ISOPE2011), Maui, Hawaii, USA, 104-112.